THE JOURNAL OF PHYSICAL CHEMISTRY

Universitat d'Alacant
Universidad de Alicante

Article

Bis(arylene-ethynylene)-*s*-Tetrazines: A Promising Family of *n*-Type Organic Semiconductors?

Monica Moral Muñoz, Andres Garzon, Yoann Olivier, Luca Muccioli, Juan-Carlos Sancho-García, Jose Manuel Granadino-Roldan, and Manuel Fernández-Gómez

J. Phys. Chem. C, **Just Accepted Manuscript** • DOI: 10.1021/acs.jpcc.5b05015 • Publication Date (Web): 22 Jul 2015

ACS Publications

The Journal of Physical Chemistry C is published by the American Chemical Society. 1155 Sixteenth Street N.W., Washington, DC 20036

Bis(arylene-ethynylene)-*s*-tetrazines: A Promising Family of *n*-Type Organic Semiconductors?

*Mónica Moral,**[1,2] *Andrés Garzón,*[3] *Yoann Olivier,*[4] *Luca Muccioli,*[5] *Juan Carlos Sancho-García,*[1] *José M. Granadino-Roldán,*[6] *and Manuel Fernández-Gómez.*[6]

[1] Department of Physical Chemistry, University of Alicante, 03080, Alicante, Spain

[2] Renewable Energy Research Institute, University of Castilla-La Mancha. Paseo de la Investigación 1, 02071, Albacete, Spain.

[3] Department of Physical Chemistry, Faculty of Pharmacy, University of Castilla-La Mancha. Paseo de los Estudiantes, 02071, Albacete, Spain.

[4] Laboratory for Chemistry of Novel Materials, University of Mons, 7000, Mons, Belgium.

[5] Laboratoire de Chimie des Polymères Organiques, UMR 5629, University of Bordeaux, 33607, Pessac, France

[6] Department of Physical and Analytical Chemistry, Faculty of Experimental Sciences, University of Jaén. Campus las Lagunillas, 23071, Jaén, Spain.

Corresponding author: monica.moral@uclm.es

ABSTRACT

We theoretically describe in this work the *n*-type semiconducting behavior of a set of bis(arylene-ethynylene)-*s*-tetrazines ($(ArCC)_2Tz$), by comparing their electronic properties with those of their parent diaryl-*s*-tetrazines (Ar_2Tz) after the introduction of ethynylene bridges. The significantly reduced internal reorganization energy for electron transfer is ascribed to an extended delocalization of the LUMO for $(ArCC)_2Tz$ as opposite to that for Ar_2Tz, which was described mostly localized on the *s*-tetrazine ring. The largest electronic coupling and the corresponding electron transfer rates found

for bis(phenyl-ethynylene)-*s*-tetrazine, as well as for some halogenated derivatives, are comparable to those reported for the best performing *n*-type organic semiconductors materials such as diimides and perylenes. The theoretical mobilities for the studied compounds turn out to be in the range 0.3 – 1.3 $cm^2\ V^{-1}\ s^{-1}$, close to values experimentally determined for common *n*-type organic semiconductors used in real devices. In addition, ohmic contacts can be expected when these compounds are coupled to metallic cathodes such as Na, Ca and Sm. For these reasons, the future application of semiconducting bis(phenyl-ethynylene)-*s*-tetrazine and its fluorinated and brominated derivatives in optoelectronic devices is envisioned.

INTRODUCTION

Tetrazine derivatives represent the most electron-deficient aromatic family[1-3] and exhibit interesting semiconducting and opto-electronic properties such as redox reversibility on reduction at low potentials[2-4,5] and a characteristic $n \rightarrow \pi^*$ low energy transition,[5-8] which can be exploited in the fabrication of OLEDs,[9] OFETs,[10] and solar cells.[11,12] *N*-type semiconducting properties have been profusely studied either for 3,6-diphenyl-*s*-tetrazine (Ph_2Tz, see Chart 1) and other diaryl-*s*-tetrazines (Ar_2Tz).[3,4,7,8,13-17] An essential drawback of Ar_2Tz to suitably act as a *n*-type organic semiconductor concerns the localized character of the Lowest Unoccupied Molecular Orbital (LUMO) which does not allow an easy accommodation of an extra electron (see Figure 1).[8,16,17] In the framework of Marcus theory for charge transfer, typically employed to describe the hopping-like charge transport in molecular crystals at room temperature[18] (vide infra), this situation gives rise to a high electron reorganization energy (λ_i). Hence the improvement of the electron transport properties of Ar_2Tz derivatives might thus rely on a decrease of the reorganization energy needed to accommodate that incoming charge.[17]

The electron transfer rate critically depends on this reorganization energy, as well as on the electronic coupling between donor and acceptor interacting molecules. Actually for some Ar_2Tz halogenated derivatives, the calculated electronic coupling values appear to be of the same order of magnitude than those reported before for the best naphthalene diimide[19] and perylene *n*-type semiconductors, [20,21] which have been successfully used in electronic devices.[22-26] Nevertheless, the high values of internal reorganization energy (λ_i) predicted for those Ar_2Tz derivatives might preclude their use as reliable semiconducting materials.[17] The increase in the delocalization of the LUMO orbital could be achieved by the introduction of ethynylene groups (–C≡C–) as a bridge between the three aromatic rings; in fact the ethynylene group, due to its axial symmetry, could allow to extend the conjugation to adjacent arylene groups.[27–32] Note also that the actual synthesis of *s*-tetrazine ethynylene derivatives is possible through cross-coupling reactions on some *s*-tetrazine compounds (compounds a and b in Chart 1), as shown by Novák and Kotschy,[33] though we are not aware of any attempt for $(ArCC)_2Tz$ compounds.

For those reasons, we aim thereby to explore the electronic properties of this new family of potential *n*-type semiconducting compounds based on bis(arylene-ethynylene)-*s*-tetrazine structures, $(ArCC)_2Tz$ (see also Chart 1).

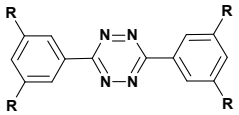

Ar_2Tz

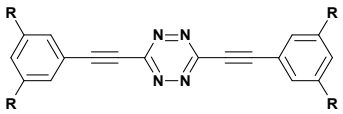

$(ArCC)_2Tz$

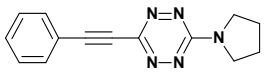

a

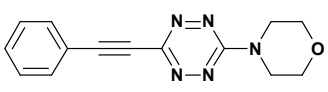

b

R = H	Ph_2Tz	R = H	$(PhCC)_2Tz$
R = F	$(F_2Ph)_2Tz$	R = F	$(F_2PhCC)_2Tz$
R = Cl	$(Cl_2Ph)_2Tz$	R = Cl	$(Cl_2PhCC)_2Tz$
R = Br	$(Br_2Ph)_2Tz$	R = Br	$(Br_2PhCC)_2Tz$

R = CN $[(CN)_2Ph]_2Tz$ R = CN $[(CN)_2PhCC]_2Tz$

Chart 1. Chemical structures of diphenyl-*s*-tetrazine derivatives, bis(phenyl-ethynylene)-*s*-tetrazine derivatives and related synthetic precursors as phenyl-ethynylene-*s*-tetrazines derivatives (*a* and *b*).

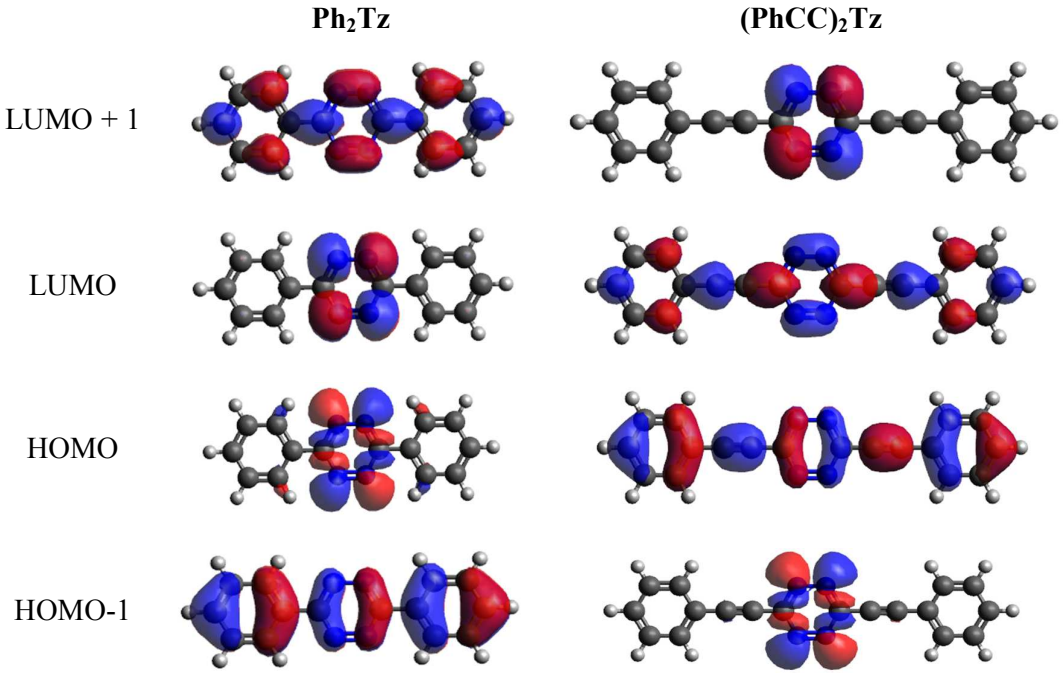

Figure 1. Shape (isocontour plots) of the frontier orbitals of Ph_2Tz (left, References 8, 17) and $(PhCC)_2Tz$ (right, this work), calculated at the B3LYP/6-31+G* level, in which the size and colours of the orbital lobes are related to their amplitude and sign, respectively.

THEORETICAL METHODOLOGY

Typically charge motion in π-conjugated organic crystal materials, due to small bandwidths (electronic couplings << 1 eV) at room temperature and strong electron-phonon coupling, is generally assisted by a hopping mechanism, which can be described within the framework of Marcus-Levich-Jortner (MLJ) model as a self-exchange electron-transfer (ET) reaction between neighboring molecules of the lattice.[34,35] Accordingly, the rate constant (k_{ET}) for this process can be expressed as:

$$k_{ET} = \frac{4\pi^2}{h} t_{12}^2 \sqrt{\frac{1}{4\pi\lambda_s k_B T}} \sum_{n=0}^{\infty} \left[exp(-S_{eff}^n) \times \frac{S_{eff}^n}{n!} \times exp\left(\frac{-(\lambda_s + n\hbar\omega_{eff} + \Delta G^0)^2}{4\lambda_s k_B T} \right) \right] \quad (1)$$

where k_B and h are Bolztmann's and Planck's constants, respectively; T is the temperature, fixed at 300 K; ΔG^0 is the free energy difference between the electronic states involved in the charge transfer process (equal to zero for an ideal self-exchange process); t_{12} stands for the electronic coupling (also called charge transfer integral) and λ_s for the "solvent" contribution to the reorganization energy, respectively. Generally speaking, in organic molecular crystals the outer contribution λ_s is of the order of one tenth of eV,[36,37] contrarily to charge transfer in solution wherein the external part might dominate,[37-42] and is fixed here at 0.1 eV. Conversely, the internal reorganization energy λ_i is calculated at the Density Functional Theory (DFT) levels and enters into equation (1) through the Huang-Rhys factor $S_{eff} = \lambda_i/\hbar\omega_{eff}$, with ω_{eff} being the frequency of an effective vibrational mode assisting the hopping process, fixed here at $\hbar\omega_{eff} \sim 0.2$ eV. Note that λ_i consists of two terms corresponding to the geometry relaxation energies upon going from the neutral-state geometry to the charged-state one and *vice versa* (Nelsen's four-point method).[43,44]

$$\lambda_i = \lambda_1 + \lambda_2 \quad (2)$$

$$\lambda_1 = E^0(G^*) - E^0(G^0) \quad (3)$$

$$\lambda_2 = E^*(G^0) - E^*(G^*) \quad (4)$$

where $E^0(G^0)$ and $E^*(G^*)$ are the ground-state energies of the optimized neutral and ionic states, respectively, $E^0(G^*)$ is the energy of the neutral molecule at the optimal ionic geometry, and $E^*(G^0)$ is the energy of the ionic state at the optimal geometry of the neutral molecule.[39-42]

The transfer integral is defined by the matrix element:

$$t_{12} = \langle\psi_1|\hat{H}|\psi_2\rangle \quad (5)$$

where $\hat{H}$ is the one-electron Hamiltonian of the system, and ψ_1 and ψ_2 are the wavefunctions of the initial and final charge-localized states.[18,42,45] The charge transfer

integral reflects the strength of the electronic interactions between pairs of molecules in the crystal and thus critically depends on their relative supramolecular arrangement. The charge transfer integral is calculated within the fragment approach at the DFT level as implemented in the Amsterdam Density Functional (ADF) package.[46] In this approach, the orbitals of the dimer are expressed as a linear combination of the molecular orbitals of the individual units (*i.e.*, fragments) that are obtained solving the Kohn-Sham equations. Since the fragment orbitals form a non-orthogonal basis set, the corresponding transfer integral depends on the choice of the energy origin so that the transfer integral is no longer an invariant. The problem is solved by applying a Löwdin transformation to the initial electronic Hamiltonian and the transfer integral t_{12} is finally obtained:

$$t_{12} = \frac{\tilde{t}_{12} - \frac{1}{2}(\varepsilon_1 + \varepsilon_2) S_{12}}{1 - S_{12}^2} \qquad (6)$$

where $\tilde{t}_{12}$, ε_i, S_{12} are the transfer integral ($<\psi_1|\hat{H}|\psi_2>$), the site energies ($<\psi_i|\hat{H}|\psi_i>$) and the overlap matrix element ($<\psi_1|\psi_2>$) defined in the non-orthogonal basis set.

For an *n*-dimensional, spatially isotropic system, where homogeneous charge diffusion can be assumed, the diffusion coefficient for charge-carries (*D*) can be evaluated as:

$$D = \frac{1}{2n} \lim_{t \to \infty} \frac{\langle [r(t) - r(0)]^2 \rangle}{t} \approx \frac{1}{2n} \sum_i r_i^2 \, k_i p_i \qquad (7)$$

where *i* runs over all nearest adjacent molecules, *n* is the dimensionality of the process while r_i and k_i are the corresponding center-to-center hopping distance and the electron transfer rate constant obtained from equation (1), respectively, with $p_i = k_i / \sum_j k_j$ as the hopping probability to the *i*-th neighbour.[45,47,24] Since the crystal structure of the studied molecules is unknown, this work focuses on the study of the charge transport

along an ideal one dimensional stack with spacing d (n = 1, p_i = ½, $D = \frac{1}{2}d^2k_{ET}$). Hence, in the zero field limit, the charge carrier mobility (μ_{hop}) can be obtained from Einstein's relation:

$$\mu_{hop} = \frac{eD}{k_BT} = \frac{e\,d^2k_{ET}}{2\,k_B\,T}. \quad (8)$$

where e is the elementary charge and d is the center-to-center distance for the π-stacked dimer, calculated as $d=(x^2+y^2+z^2)^{1/2}$, where x, y and z are the displacements along the three directions defined in Figure 2.[45,47,24]

The electron injection efficiency from an electrode to the *s*-tetrazine derivatives is estimated by considering two key physical properties: (i) the energy difference between the LUMO level (E_{LUMO}) of the organic semiconductor and the work function (Φ) of the electrode. The metal-semiconductor interface is usually treated as a Mott-Schottky barrier, where the barrier height is given by the difference between Φ and the semiconductor HOMO or LUMO level.[38,48] Although in this ideal model interfacial effects between electrode and semiconductor are not taken into account,[37] the comparison of Φ with HOMO/LUMO levels of the semiconductor helps to find out the likeliness of charge injection and the magnitude of the contact resistance; (ii) the electron affinity (EA) defined as the energy released when one electron is added to the system in the gaseous state. EA of a semiconductor should amount at least to 3.0 eV for an easy electron injection.[38,49] However, its stability in ambient conditions could be compromised by high EA values as well as other factors as the crystal packing and film morphology.[38,50-52] The adiabatic (AEA) and vertical (VEA) electron affinity were calculated as follows

$$AEA = E_0(G_0) - E^*(G^*) \quad (9)$$

$$VEA = AEA + \lambda_2 \quad (10)$$

where $E_0(G_0)$, $E^*(G^*)$ and λ_2 are the same quantities appearing in equations (3) and (4).

COMPUTATIONAL METHODS

With the purpose of achieving the best tradeoff between accuracy and computational cost, we have performed Density Functional Theory (DFT) calculations with the well-established and widely used B3LYP[53,54] and M06-2X[55] functionals, as implemented in Gaussian09 (revision **B.01**).[56] Geometries were optimized at the B3LYP/6-31+G* level, and the nature of the minima was confirmed by means of the eigenvalues (all positive) of the corresponding Hessian matrices. The M06-2X/6-31G* model chemistry was used for the calculation of the binding energy for $(ArCC)_2Tz$ dimers, defined as the energy difference between the dimer and the isolated molecules. On the one hand, we have calculated the binding energy for two molecules that we have kept with face-to-face planes at a distance of 3.4 Å along z-direction (see Figure 2), corresponding to a typical π-stacking distance. While the position of one of the molecules was kept fixed, the second molecule was displaced along x- and y-axes in a grid of 0.2 Å in both directions. In addition, we have calculated the binding energy as a function of the z-axis displacement, fixing x- and y-axes to the values giving the lowest binding energy in the previous (x,y) energy scan. Although traditional DFT functionals perform poorly for non-covalent interactions, the M06 family of functionals has been shown to give reasonably accurate stacking geometries for a variety of dispersion-dominated systems, such as perylenediimides and quaterthiophenes,[57,58] as well as DNA base pairs,[59] and aromatic systems used as organic semiconductors, such as quaterthiophene, in which the electronic coupling and binding energies calculated at M06-2X level yield similar results to those obtained with other (dispersion-corrected) functionals like PBE0-dDsC/def2-SVP.[58] The transfer integral t_{12} was calculated with the B3LYP functional and the double zeta polarized (DZP) basis set, while the

remaining key electronic properties (E_{LUMO}, EA, λ_i) were calculated at the B3LYP/6-31+G* level of theory. Although Koopmans theorem is not rigorously applicable to Kohn-Sham orbital energies, Perdew proved a connection between ionization potentials/electron affinities and HOMO/LUMO energies through Janak's theorem (see, e.g. ref. 60-62 and references therein). In this sense, B3LYP has been proven to be accurate enough for predicting EAs[63,64] and provides theoretical λ_i values in good quantitative agreement with the experimental ones from gas-phase ultraviolet photoelectron spectroscopy.[65] Zhang and Musgrave have also reported that B3LYP yields lower errors in the LUMO energy of small organic molecules as compared to other DFT methods with a higher percentage of Hartree-Fock exchange.[66] The 6-31+G* basis set is recommended in calculations involving anionic species and was therefore used here.[62]

The spatial variation of the electron coupling has been scanned as a function of the x- and y-axes displacement at fixed z = 3.4 Å. In addition, t_{12} has been calculated for different configurations of the molecules considered in this study corresponding to a minimum in the binding energy.

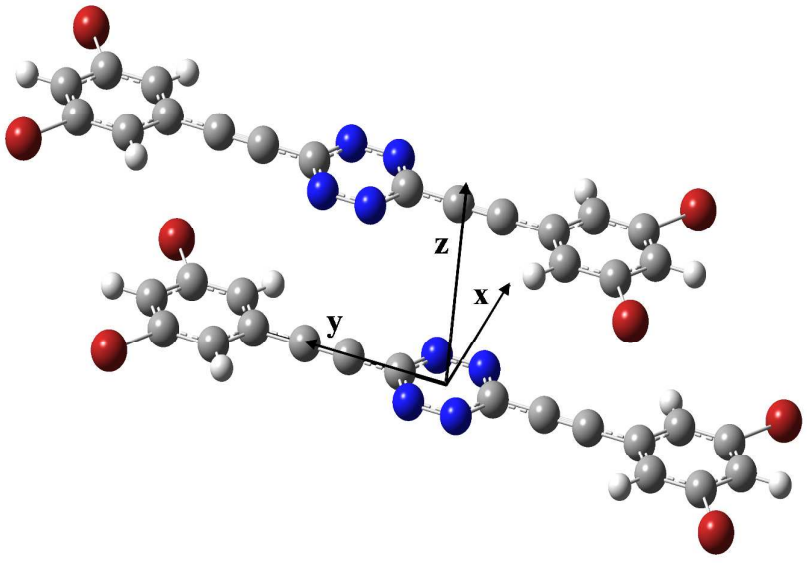

Figure 2. $(Br_2PhCC)_2Tz$ dimer in the position x = 2.0 Å, y = 3.4 Å and z = 3.4 Å, where (x,y,z) is the relative displacement between the tetrazine units along the short (x) and long (y) molecular axes, and the π-stacking direction (z).

RESULTS AND DISCUSSION

The internal reorganization energies (λ_i) previously reported for a set of Ar_2Tz derivatives lie in the range 0.48 – 0.62 eV [17] *i.e.* about twice the values obtained for typical *n*-type organic semiconductors such as perfluoropentacene (0.24 eV),[39] diimides (0.22 – 0.35 eV),[24] fluoroarene-oligothiophenes (0.22 – 0.34 eV)[67] and core-twisted chlorinated perylene bisimide (0.30 – 0.34).[68] However, the presence of the ethynylene bridges in $(ArCC)_2Ph$ derivatives substantially lowers λ_i to values comparable to those reported for the above mentioned reference compounds (see Table 1). The decrease of λ_i is closely related to the change in the shape of the LUMO, which becomes completely delocalized for $(ArCC)_2Tz$ (see Figure 1 for $(PhCC)_2Tz$). In addition, we have observed a cross correlation between the shapes of the LUMO and LUMO + 1 orbitals for Ph_2Tz and $(PhCC)_2Tz$. Similar correlation is also observed for the HOMO and HOMO-1 orbitals (see Figure 1).

Table 1. Internal reorganization energy (λ_i) for $(Ar_2CC)_2Tz$ derivatives (this work) and for Ar_2Tz (ref. 17). Calculations were carried out at the B3LYP/6-31+G* level.

Compounds	λ_1/ eV	λ_2/ eV	λ_i / eV	Compounds	λ_1/ eV	λ_2/ eV	λ_i/ eV
Ph_2Tz	0.30	0.29	0.60	$(PhCC)_2Tz$	0.10	0.12	0.22
$(F_2Ph)_2Tz$	0.22	0.31	0.53	$(F_2PhCC)_2Tz$	0.11	0.16	0.27
$(Cl_2Ph)_2Tz$	0.31	0.30	0.61	$(Cl_2PhCC)_2Tz$	0.13	0.13	0.26
$(Br_2Ph)_2Tz$	0.31	0.31	0.62	$(Br_2PhCC)_2Tz$	0.14	0.12	0.26
$(CN_2Ph)_2Tz$	0.26	0.23	0.48	$(CN_2PhCC)_2Tz$	0.11	0.12	0.23

The electron transfer rate also strongly depends on electronic coupling values, which reveals the strength of the electronic interactions between neighboring molecules, and thus critically depends on the relative spatial arrangement in the bulk. However, to

the best of our knowledge, these compounds have not been synthetized yet. Therefore, X-ray structures are not available for any of the $(ArCC)_2Tz$ compounds; consequently, in order to use a plausible crystal structure in the calculations, the arrangement of every pair of molecules is modeled assuming a stacked disposition typical for similar Ar_2Tz systems.[17,69,70] Based on these structures, the transfer integrals are corresponding computed.

Also the binding energy is calculated for stacking dimers as a function of the relative (x,y) displacement between both molecules keeping z fixed at 3.4 Å. A large number of energetically accessible stacking geometries are considered (see Figure 3). For all the compounds, a broad minimum appears for x- and y-displacements lower than 2 Å and the binding energy reaches a maximum value for the fully overlapped dimer. A second minimum, placed at $x \approx 3 - 4$ Å and $y < 1$ Å, is also observed for all of them with the exception of the brominated derivative. A complex landscape with up to four energy valleys is observed for $(PhCC)_2Tz$. The position of the global minimum in the binding-energy landscape is found by displacing the molecules along the long axis direction ($x \sim 0$, $y = 1.4 - 1.6$ Å) for $(Br_2PhCC)_2Tz$ and $(NC_2PhCC)_2Tz$, while the global minimum for the rest of compounds is placed along the x-displacement ($x = 1.2 - 3.4$ Å). In general, we found that the binding energies minima are located inside the region $1 < (x^2+y^2)^{1/2} < 2$ (see Figure 3) with the exception of $(PhCC)_2Tz$. Once the global minima are localized on the energy landscapes, the binding energy was also monitored as a function of the z-displacement being $z = 3.2$ Å the displacement that mostly lowers it (see Figure 4). The largest (minimum) binding energy was obtained for $(Br_2PhCC)_2Tz$, ~ -1.4 eV, about twice as large as that for the rest of compounds (see Table 2).

Table 2. Largest binding energy ($E_{b,min}$) and the corresponding relative x,y,z-positions of the molecules within stacked dimers of the $(ArCC)_2Tz$ family studied here. Charge transfer integral, t_{12} transfer rates k_{ET}, mobility and relative mobility with respect to $(PhCC)_2Tz$ calculated from equation (8) at the corresponding dimer geometries.

Compound	$E_{b,min}$ / eV	x / Å	y / Å	z / Å	t_{12} / meV	k_{ET} / s^{-1}	μ / V^{-1} cm^2 s^{-1}	μ_{rel}
$(PhCC)_2Tz$	-0.648	0.0	3.4	3.2	74	3.67×10^{13}	0.727	1.000
$(F_2PhCC)_2Tz$	-0.712	0.6	1.2	3.1	48	1.20×10^{13}	0.266	0.365
$(Cl_2PhCC)_2Tz$	-0.798	0.0	1.6	3.3	24	3.16×10^{12}	0.082	0.113
$(Br_2PhCC)_2Tz$	-1.389	1.4	0.0	3.3	99	5.38×10^{13}	1.337	1.839
$(CN_2PhCC)_2Tz$	-0.777	1.6	0.6	3.2	1	6.38×10^{9}	0.0001	0.0002

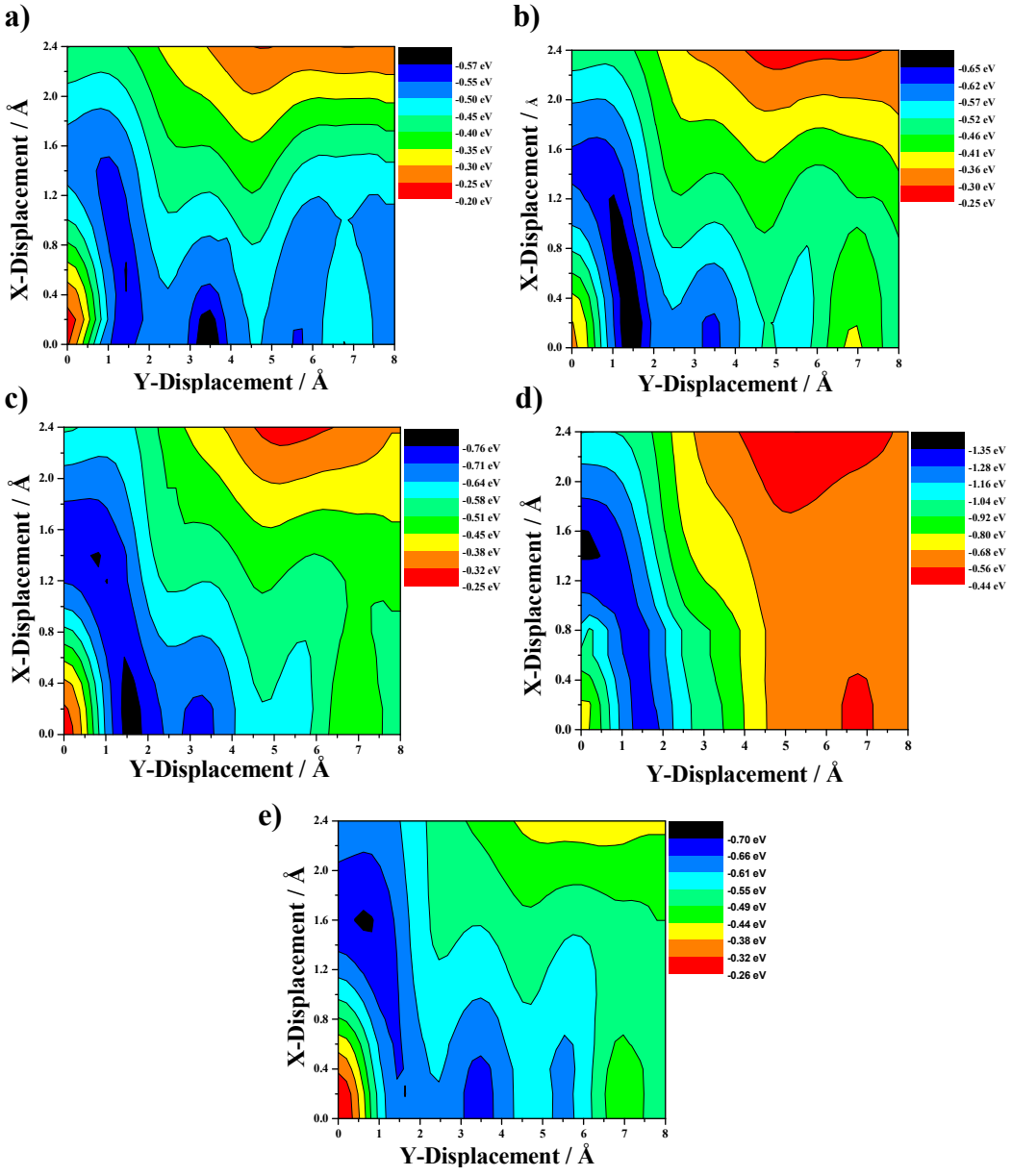

Figure 3. Binding energy for a) $(PhCC)_2Tz$; b) $(F_2PhCC)_2Tz$; c) $(Cl_2PhCC)_2Tz$; d) $(Br_2PhCC)_2Tz$ and e) $(CN_2PhCC)_2Tz$ dimers *vs.* stacking geometry (z = 3.4 Å).

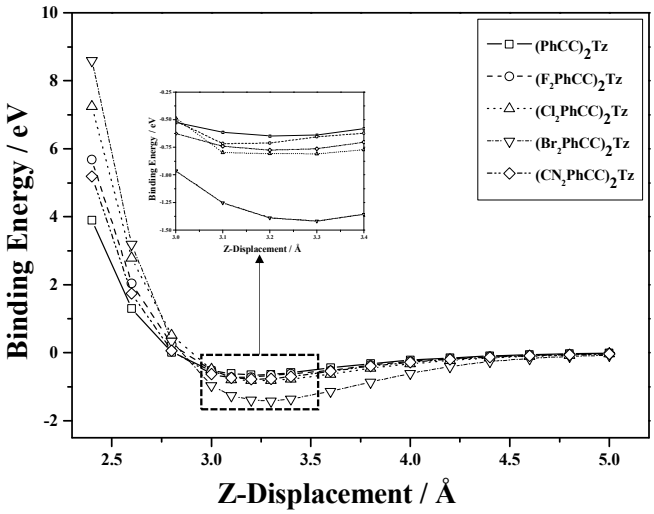

Figure 4. Binding energy dependence as a function of the z-displacement for the $(PhCC)_2Tz$, $(F_2PhCC)_2Tz$, $(Cl_2PhCC)_2Tz$, $(Br_2PhCC)_2Tz$ and $(CN_2PhCC)_2Tz$ dimers.

Unexpectedly, the highest values of binding energies are observed for slightly displaced geometries (see Table 2) rather than for those at a perfectly cofacial disposition (at x = y = z = 0 Å, see Figure 5), allowing us to conclude that nuclear repulsion dominates the binding energy landscapes in this region (Figure 3). Coming back to Table 2, which collects the t_{12} values calculated for the arrangements with the lowest binding energies, we can observe that the largest electronic coupling is obtained for $(Br_2PhCC)_2Tz$ (99 meV) followed by $(PhCC)_2Tz$ (74 meV) and $(F_2PhCC)_2Tz$ (48 meV). All these values are larger than those calculated for Ph_2Tz, $(F_2Ph)_2Tz$ and $(Br_2Ph)_2Tz$ crystals (18, 45 and 51 meV, respectively) previously studied.[17] In general, t_{12} values calculated for $(PhCC)_2Tz$, $(F_2PhCC)_2Tz$ and specially $(Br_2PhCC)_2Tz$ are close to those reported for oligoacenes including pentacene (131 meV calculated at the

B3LYP/TZP level),[46] for the perylene derivatives studied by Wang et al. (26 − 64 meV, calculated at the PW91PW91/6-31G* level),[25] for the sets of diimides derivatives studied by Chen et al. (21.6 − 87.5 meV, calculated at the PW91PW91/6-31G* level)[24] and by Di Donato et al. (74 − 96 meV, calculated at the B3LYP/3-21G level).[26]

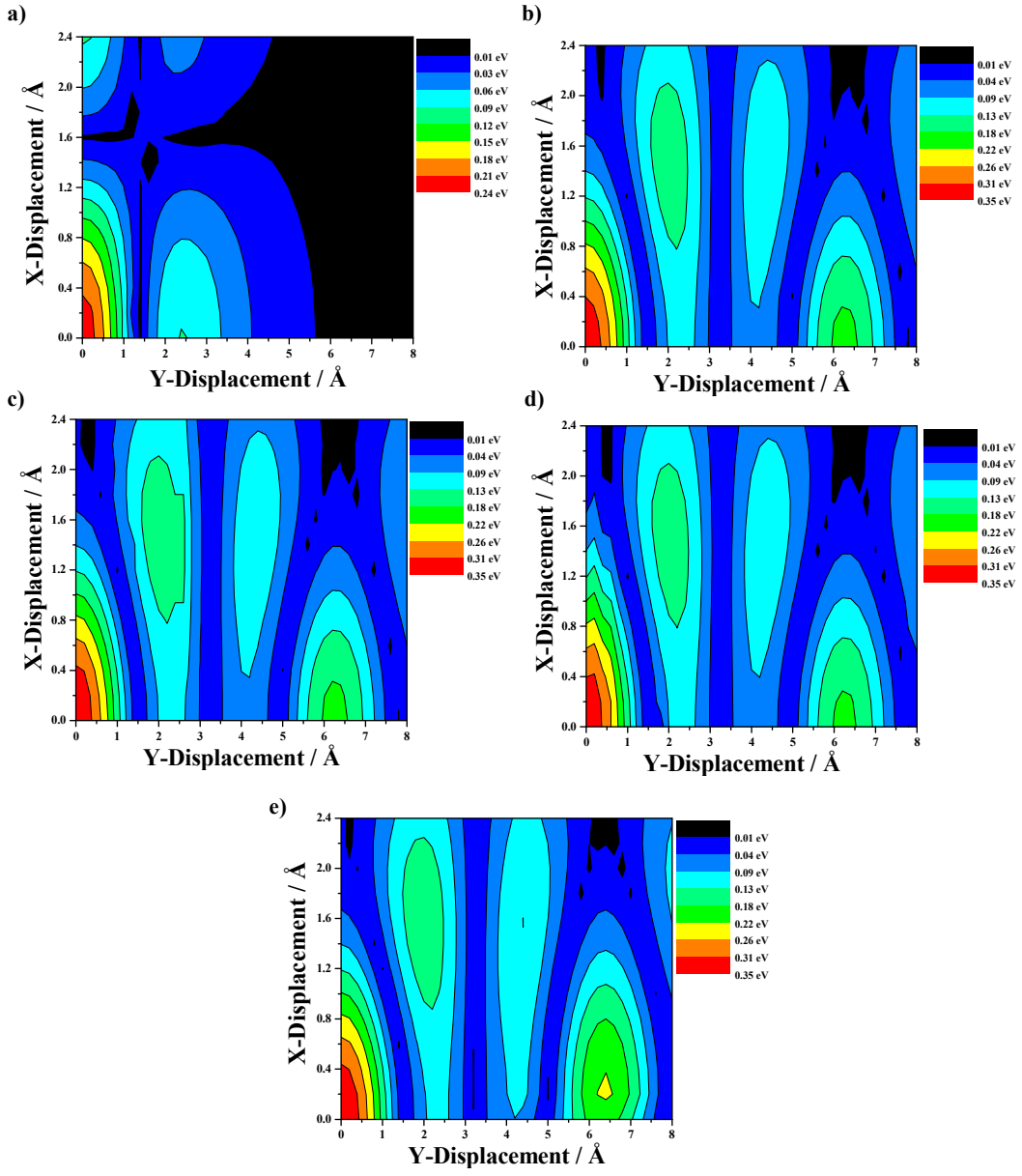

Figure 5. Electron couplings for a) $(PhCC)_2Tz$; b) $(F_2PhCC)_2Tz$; c) $(Cl_2PhCC)_2Tz$; d) $(Br_2PhCC)_2Tz$ and e) $(CN_2PhCC)_2Tz$ dimers *vs*. stacking geometry (z = 3.4 Å) as surface plot.

When comparing the molecules studied here with the tetrazine derivatives previously published,[17] we observe the highest k_{ET} and μ values were obtained for $(PhCC)_2Tz$ and its brominated and fluorinated derivatives, which have mobilities (0.30 − 1.34 $cm^2\ V^{-1}\ s^{-1}$) at least one order of magnitude higher than those reported for the corresponding parent compounds Ph_2Tz, $(F_2Ph)_2Tz$ and $(Br_2Ph)_2Tz$ (~ 0.006 − ~ 0.026 $cm^2\ V^{-1}\ s^{-1}$) at the same level of theory.[17] Similar values of electron mobilities have been calculated for sets of perylene dibisimide derivatives (0.007 − 1.45 $cm^2\ V^{-1}\ s^{-1}$),[71] tetracarboxylic diimide derivatives (0.08 and 0.34 $cm^2\ V^{-1}\ s^{-1}$)[72] and core-twisted chlorinated perylene bisimide (0.004 – 0.28 $cm^2\ V^{-1}\ s^{-1}$)[68] employing the MLJ formulation. Mobilities estimated for $(PhCC)_2Tz$, $(F_2PhCC)_2Tz$ and $(Br_2PhCC)_2Tz$ lie close to the range of the values experimentally determined for common *n*-type organic semiconductors. For instance, experimental μ values measured under vacuum for electron-deficient N,N'-substituted arylenediimides and perfluoroalkyl oligothiophenes turn out to be in the ranges of 0.02 – 0.35 and 0.03 – 1.7 $cm^2\ V^{-1}\ s^{-1}$, respectively.[73] The OFET performances of bis(thienyl)-*s*-tetrazine bridged to naphthalene diimide moieties have been recently studied (μ values within 0.005 – 0.14 $cm^2\ V^{-1}\ s^{-1}$ were reported) showing the potential of *s*-tetrazine derivatives as *n*-type semiconductors.[74] Nevertheless, we must emphasize that the comparison between experimental and theoretical mobilities is far from trivial due to some assumptions in the theoretical model, in particular the geometry chosen for the calculation, together with other experimental factors (for example, traps) intrinsically difficult to be taken into account. However, without trying to reproduce the absolute experimental values, the results show an undeniable comparative characteristic.

The performance of an organic semiconductor device does not only depend on the bulk charge mobility of the semiconducting material but also on the efficiency of the electron injection at the electrodes. The interface between metal (cathode) and *n*-type organic semiconductor is usually treated as a Mott-Schottky barrier, where the barrier height is given by the difference between the metal work function (Φ) and the (gas) semiconductor LUMO level (E_{LUMO}).[38] A good ohmic contact between semiconductor materials and electrodes is generally expected only for potential barriers lower than 0.2 − 0.3 eV,[75,76] while for larger barriers interfacial effects such as metal reactivity, polarization processes and inter-diffusion within the metal-organic interface and temperature cannot be neglected.[38,77-79] For this reason, the sole analysis of Φ and E_{LUMO} values cannot provide a quantitative evaluation of the injection barrier but it nevertheless serves as a guide to predict the alignment of levels at the interface and the electron injection barrier, as well as to interpret trends within a set of related compounds.[48,79-81] Figure 6 shows the calculated E_{LUMO} for the set of $(ArCC)_2Tz$ and their corresponding parent compounds, Ar_2Tz. This figure also collects reduction potentials recently reported for some aryl-*s*-tetrazine derivatives (shown in Figure 7) and their E_{LUMO} estimated by using of an empirical equation proposed by De Leeuw et al.[82] The introduction of ethynylene bridges produces an increase within 0.3 – 0.6 eV in E_{LUMO} with respect to the corresponding parent compounds. Even so, E_{LUMO} values calculated for $(ArCC)_2Tz$, excepting only $(PhCC)_2Tz$, are comparable to those estimated for other aryl-*s*-tetrazine derivatives. In this sense, the presence of halogen atoms and especially cyanide groups in the $(ArCC)_2Tz$ compounds significantly lowers E_{LUMO} with respect to $(PhCC)_2Tz$ which should bring on a more efficient charge injection[38,49,52,83] and could also help the environmental stability of the material.[52,84] Interestingly, E_{LUMO} is decreased by 0.4 – 0.5 eV with respect to $(PhCC)_2Tz$ due to the

presence of four halogen atoms and *ca.* 1.1 eV by the inclusion of the cyanide groups, reaching a minimum value of - 3.68 eV. Energy barriers, Φ - $|E_{LUMO}|$, lower than 0.3 eV were calculated for all the studied compounds with respect to some common electrodes used for electron injection, *i.e.* Na (Φ = - 2.6 eV), Ca (Φ = - 2.8 eV eV) and Sm (Φ = - 2.7 eV).[85-89] Furthermore, ohmic contact is also expected for $(CN_2PhCC)_2Tz$ with respect to the Mg electrode (Φ = - 3.2 eV).[88,90]

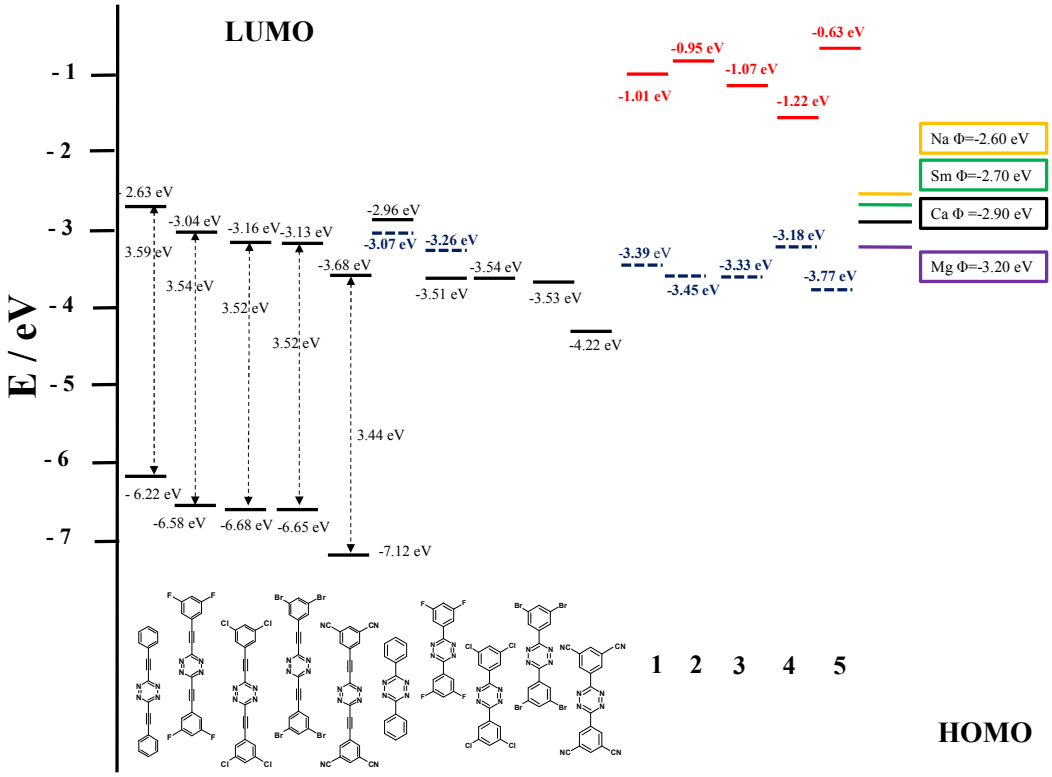

Figure 6: Experimental reduction potentials (red lines) and corresponding LUMO energies (blue dashed lines) estimated with the empirical equation (E_{LUMO} = -[E_{red} + 4.4] eV; reference 82) are shown. Calculated LUMO energies for the parents compounds (reference 17) at B3LYP/6-31+G* level and LUMO and HOMO energies evaluated at the B3LYP/6-31+G* level for the series of $(ArCC_2)Tz$ derivatives studied here. The values for aryl-*s*-tetrazine derivatives **1-5** (see Figure 7) have been extracted from references 74 and 91-93.

Electron injection efficiency is also related to vertical electron affinity, VEA, which increases between 0.2 and 0.4 eV with respect to Ar_2Tz derivatives, due to the presence of the ethynylene groups (see Table 3).[17] The adiabatic electron affinity, AEA, also increases of 0.5 – 0.6 eV for the tetrahalogenated derivatives and 1.1 eV for the cyanide derivative with respect to $(PhCC)_2Tz$, with AEA consistently larger of about 0.1 – 0.2 eV for $(ArCC)_2Tz$ compounds as compared to Ar_2Tz. This observation is in agreement with some literature results and with chemical intuition, suggesting that the addition of electron-withdrawing substituents to the aromatic cores increases the electron affinity values, as well as the air stability of the electron-transporting materials.[22] For instance, Kuo et al. have observed that the introduction of a few CN groups in pentacene raises the EA to values even larger than those of perfluoropentacene.[83]

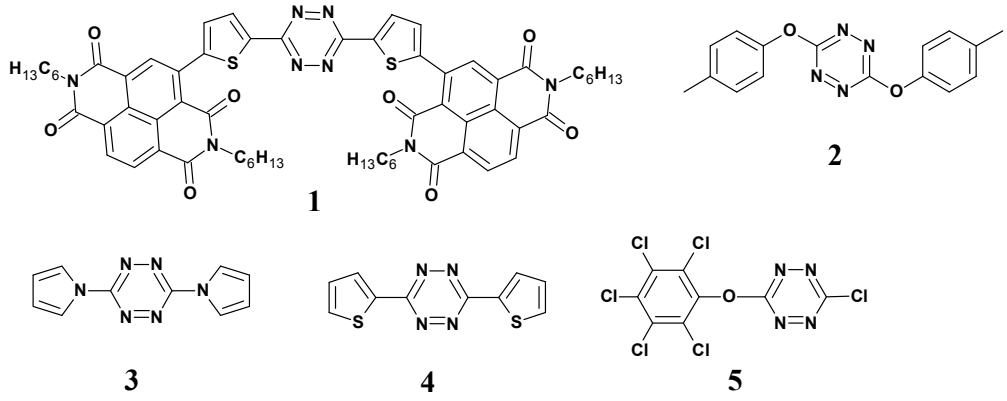

Figure 7. Chemical formulae of the *s*-tetrazine derivatives mentioned in Figure 6.

Table 3. Adiabatic (AEA) and vertical (VEA) electron affinity calculated at B3LYP/6-31+G* level for $(ArCC)_2Tz$ and comparison with the values reported for their parent compounds, Ar_2Tz (Reference 17).

Compounds	AEA / eV	VEA / eV	Compounds	AEA / eV	VEA / eV
Ph_2Tz	1.51	1.22	$(PhCC)_2Tz$	1.78	1.66
$(F_2Ph)_2Tz$	2.16	1.84	$(F_2PhCC)_2Tz$	2.28	2.13
$(Cl_2Ph)_2Tz$	2.15	1.85	$(Cl_2PhCC)_2Tz$	2.34	2.20
$(Br_2Ph)_2Tz$	2.17	1.86	$(Br_2PhCC)_2Tz$	2.35	2.22

$(CN_2Ph)_2Tz$	2.86	2.63	$(CN_2PhCC)_2Tz$	2.92	2.80

CONCLUSIONS

The electronic properties of the *n*-type semiconducting bis(arylene-ethynylene)-*s*-tetrazine, $(ArCC)_2Tz$ derivatives were theoretically studied employing state-of-the-art DFT calculations. These compounds might promisingly be applied in real devices. In fact, we note first that the reorganization energies calculated for $(ArCC)_2Tz$ derivatives are substantially lower than those reported for their parent compounds, Ar_2Tz, studied previously.[17] The change in the shape of the LUMO, which is completely delocalized for $(ArCC)_2Tz$ and localized on the Tz ring for Ar_2Tz is the origin of this difference. Indeed the λ_i values calculated for $(ArCC)_2Tz$ compounds are comparable to those reported for typical *n*-type organic semiconductors such as perfluoropentacene, diimides and fluoroarene-oligothiophenes.[24,39,67] The second reason for stimulating practical applications is that the electronic couplings t_{12}, calculated for the dimers at the lowest binding energy geometry, are rather large, with $(Br_2PhCC)_2Tz$, $(PhCC)_2Tz$ and $(F_2PhCC)Tz$ showing the largest electronic couplings, again higher than those calculated for their parent compounds,[17] and comparable to the values reported for different diimides and perylenes with assessed *n*-type semiconductor character.[24-26] Also the electron mobilities estimated for these compounds are in line with the values reported for perylene bisimide derivatives and tetracarboxylic diimide derivatives[71,72] and lie on the range of the values experimentally determined for common *n*-type organic semiconductors such as N,N'-substituted arylenediimides and perfluoroalkyl oligothiophenes.[73] Regarding electron injection, ohmic contact can be expected for all the studied $(ArCC)_2Tz$ derivatives with respect to some of the common electrodes used

for electron injection such as Na, Ca and Sm. Therefore, $(PhCC)_2Tz$, $(F_2PhCC)Tz$ and particularly $(Br_2PhCC)_2Tz$ might be considered as promising compounds which could exhibit a *n*-type semiconductor character.

ACKNOWLEDGEMENTS

The research in Bordeaux has been funded by the French national grant ANR-10-LABX-0042-AMADEus managed by the National Research Agency under the initiative of excellence IdEx Bordeaux programme (reference ANR-10- IDEX-0003-02). The work in Mons was supported by the Programme d'Excellence de la Région Wallonne (OPTI2MAT project) and the Belgian National Fund for Scientific Research (FNRS-FRFC).

José M. Granadino-Roldán and Manuel Fernández-Gómez thank the Consejería de Innovación, Junta de Andalucía for their financial support (FQM337 grant).

REFERENCES

(1) Katritzky, A. *Handbook of heterocyclic chemistry*. Pergamon Press. New York. **1986**.

(2) Gong, Y. H.; Audebert, P; Tang, J; Miomandre, F; Clavier, G; Badré, S; Méallet-Renault, R; Marrot, J. New Tetrazines Substituted by Heteroatoms Including the First Tetrazine Based Cyclophane: Synthesis and Electrochemical Properties. *J. Electroanal. Chem*. **2006**, *592*, 147–152.

(3) Clavier, G; Audebert, P. *S*-tetrazine as Building Blocks for New Functional Molecules and Molecular Materials. *Chem. Rev*. **2010**, *110*, 3299–3314.

(4) Troll, T. Reduction Potentials of Substituted *S*-triazines and *S*-tetrazines in Acetonitrile. *Electrochim. Acta*. **1982**, *27*, 1311–1314.

(5) Audebert, P; Miomandre, F.; Clavier, G.; Vernières, M. C.; Badré, S.; Méallet-Renault, R. Synthesis and Properties of New Tetrazines Substituted by Heteroatoms: Towards the World's Smallest Organic Fluorophores. *Chem. Eur. J.* **2005**, *11*, 5667–5673.

(6) Plugge, M.; Alain-Rizzo, V.; Audebert, P.; Brouwer, A. M. Excited State Dynamics of 3,6-Diaryl-1,2,5,6-tetrazines. Experimental and Theoretical Studies. *J. Photochem. Photobiol. A: Chem*. **2012**, *234*, 12–20.

(7) Kaim, W. The Coordination Chemistry of 1,2,5,6-Tetrazines. *Coord. Chem. Rev.* **2002**, *230*, 127–139.

(8) Moral, M.; García, G.; Peñas, A.; Garzón, A.; Granadino-Roldán, J. M.; Melguizo, M.; Fernández-Gómez, M. Electronic Properties of Diphenyl-s-tetrazine and Some Related Oligomers. A Spectroscopic and Theoretical Study. *Chem. Phys*. **2012**, *408*, 17–27.

(9) Shinar, J.; Shinar, R. Organic Light Emitting Devices (OLEDs) and OLED-based Chemical and Biological Sensors: An Overview. *J. Phys. D: Appl. Phys.* **2008**, *41*, 133001–133001.

(10) Torsi, L.; Magliulo, M.; Manoli, K.; Palazzo, G. Organic Field-effect Transistor: A Tutorial Review. *Chem. Soc. Review*. **2013**, *42*, 8612–8628.

(11) Clarke, T. M.; Durrant, J. R. Charge Photogeneration in Organic Solar Cells. *Chem. Rev.* **2010**, *110*, 6736–6767.

(12) Günes, S.; Neugebauer, H.; Saricifci, N. S. Conjugated Polymer-Based Organic Solar Cells. *Chem. Rev*. **2007**, *107*, 1324–1338.

(13) Waluk, J.; Spanget-Larsen, J.; Thulstrup, E. Electronic States of Symmetrically Disubstituted *s*-Tetrazines. *Chem. Phys*. **1995**, *200,* 201–213.

(14) Qing, Z.; Audebert, P.; Clavier, G.; Miomandre, F.; Tang, J.; Vu, T. T.; Méallet-Renault, R. Tetrazines with Hindered or Electron Withdrawing Substituents: Synthesis, Electrochemical and Fluorescence Properties. *J. Electroanal. Chem*. **2009**, *632*, 39–44.

(15) Gong, Y. H.; Miomandre, F.; Méallet-Renault, R.; Badré, S.; Galmiche, L.; Tang, T.; Audebert, P.; Clavier, G. Synthesis and Physical Chemistry of s-Tetrazines: Which Ones Are Fluorescent and Why?. *Eur. J. Org. Chem*. **2009**, 6121–6128.

(16) Moral, M.; Granadino-Roldán, J. M.; Garzón, A.; García, G.; Fernández-Gómez, M. Does the Number of Nitrogen Atoms Have an Influence on the Conducting Properties of Diphenylazines? A DFT Insight. *Chem. Phys*. **2011**, *379*, 51–56.

(17) Moral, M.; García, G.; Garzón, A.; Granadino-Roldán, J. M.; Fox, M. A., Yufit, D. S.; Peñas, A.; Melguizo, M.; Fernández-Gómez, M. Electronic Structure and Charge Transport Properties of a Series of 3,6-(Diphenyl)-*s*-tetrazine Derivatives: Are They Suitable Candidates for Molecular Electronics?. *J. Phys. Chem. C* **2014**, *118*, 26427−26439.

(18) Coropceanu, V.; Cornil, J.; da Silva Filho, D. A.; Olivier, Y.; Silvey, R.; Brédas. J. L. Charge Transport in Organic Semiconductors. *Chem. Rev*. **2007**, *107*, 926–952.

(19) Tatemichi, S.; Ichikawa, M.; Koyama, T.; Taniguchi, Y. High Mobility *n*-Type Thin-Film Transistors Based on N,N′-Ditridecyl Perylene Diimide with Thermal Treatments. *Appl. Phys. Lett*. **2006**, *89*, 112108−112110.

(20) Chesterfield, R. J.; McKeen, J. C.; Newman, C. R.; Ewbank, P. C.; da Silva Filho, D. A.; Bredas, J. L.; Miller, L. L.; Mann, K. R.; Frisbie, C. D. Organic Thin Film Transistors Based on N-Alkyl Perylene Diimides: Charge Transport Kinetics as a Function of Gate Voltage and Temperature. *J. Phys. Chem. B*. **2004**, *108*, 19281−19292.

(21) Briseno, A. L.; Mannsfeld, S. C. B.; Reese, C.; Hancock, J. M.; Xiong, Y.; Jenekhe, S.; Bao, Z.; Xia, Y. Perylenediimide Nanowires and Their Use in Fabricating Field-Effect Transistors and Complementary Inverters. *Nano Lett.* **2007**, *7*, 2847−2853.

(22) Zhou, K.; Dong, H.; Zhang, H. L.; Hu, W. High Performance *n*-Type and Ambipolar Small Organic Semiconductors for Organic Thin Film Transistors. *Phys. Chem. Chem. Phys*. **2014**, *16*, 22448−22457.

(23) Canola, S.; Negri, F. Anisotropy of the n-Type Charge Transport and Thermal Effects in Crystals of a Fluoro-Alkylated Naphthalene Diimide: A Computational Investigation. *Phys. Chem. Chem. Phys*. **2014**, *16*, 21550−21558.

(24) Chen, X. K.; Zou, L. Y.; Guo, J. F.; Ren, A. M. An Efficient Strategy for Designing *n*-Type Organic Semiconductor Materials-Introducing a Six-Membered Imide Ring into Aromatic Diimides. *J. Mater. Chem.* **2012**, *22*, 6471−6484.

(25) Wang, C.; Wang, F.; Yang, X.; Li, Q.; Shuai, Z. Theoretical Comparative Studies of Charge Mobilities for Molecular Materials: PET *vs* Bnpery. *Org. Electron.* **2008**, *9*, 635−640.

(26) Di Donato, E.; Fornari, R. P.; Di Motta, S.; Li, Y.; Wang, Z.; Negri, F. *n*-Type Charge Transport and Mobility of Fluorinated Perylene Bisimide Semiconductors. *J. Phys. Chem. B* **2010**, *114*, 5327−5334.

(27) Granadino-Roldán J. M.; Garzón, A.; García, G.; Peña-Ruiz, T.; Fernández–Liencres, M. P.; Navarro A.; Fernández-Gómez M. Theoretical Study of the Effect of Ethynyl Group on the Structure and Electrical Properties of Phenyl-Thiadiazole Systems as Precursors of Electron-Conducting Materials. *J. Chem. Phys.* **2009**, *130*, 234907−234907.

(28) Garzón, A.; Granadino-Roldán, J. M.; Moral, M.; García, G.; Fernández-Liencres, M. P.; Navarro, A.; Peña-Ruiz, T.; Fernández-Gómez, M. Density Functional Theory Study of the Optical and Electronic Properties of Oligomers Based on Phenyl-Ethynyl Units Linked to Triazole, Thiadiazole, and Oxadiazole Rings To Be Used in Molecular Electronics. *J. Chem. Phys.* **2010**, *132*, 064901–11.

(29) Beeby, A.; Findlay, K. S.; Low, F. J.; Marder, T. B.; Matousek, P.; Parker, A.W.; Rutter, S. R.; Towrie, M. Studies of the S1, State in a Prototypical Molecular Wire Using Picosecond Time-Resolved Spectroscopies. *Chem. Commun*. **2003**, 2406–2407.

(30) Beeby, A.; Findlay, K. S.; Low, F. J.; Marder, T. B. A Re-Evaluation of The Photophysical Properties of 1,4-Bis(phenylethynyl)benzene: A Model for Poly(phenyleneethynylene). *J. Am. Chem. Soc.* **2002**, *124*, 8280–8284.

(31) Greaves, S. J.; Flynn, E. L.; Futcher, F. L.; Wrede, E.; Lydon, D. P.; Low, P. J.; Rutter, S. R.; Beeby, A. Cavity Ring-Down Spectroscopy of the Torsional Motions of 1,4-Bis(phenylethynyl)benzene. *J. Phys. Chem. A.* **2006**, *110*, 2114–2121.

(32) Levitus, M.; Schmieder, K.; Ricks, H.; Shimizu, K. D.; Bunz, U. F.; Garcia-Garibay, M. A. Steps To Demarcate the Effects of Chromophore Aggregation and Planarization in Poly(phenyleneethynylene)s. 1. Rotationally Interrupted Conjugation in the Excited States of 1,4-Bis(phenylethynyl)benzene. *J. Am. Chem. Soc.* **2001**, *123*, 4259–4625.

(33) Novák, Z.; Kotschy, A. First Cross-Coupling Reactions on Tetrazines. *Org. Lett.* **2003**, *5*, 3495–3497.

(34) Marcus, R. A. Electron Transfer Reaction in Chemistry. Theory and Experiment. *Rev. Mod. Phys.* **1993**, *65*, 599–610.

(35) Barbara, P. F.; Meyer, T. J.; Ratner, M. A. Contemporary Issues in Electron Transfer Research. *J. Phys. Chem.* **1996**, *100*, 13148–13168.

(36) Martinelli, N. G.; Idé, J.; Sánchez-Carrera, R. S.; Coropceanu, V.; Brédas, J. L.; Ducasse, L.; Castet, F.; Cornil, J.; Beljonne, D. Influence of Structural Dynamics on Polarization Energies in Anthracene Single Crystals. *J. Phys. Chem. C.* **2010**, *114*, 20678–20685.

(37) McMahon, D. P.; Troisi, A. Evaluation of External Reorganization Energy of Polyacenes. *J. Phys. Chem. Lett.* **2010**, *1*, 941–946.

(38) Newman, C. R.; Frisbie, C. D.; da Silva Filho, D. A.; Brédas, J. L.; Ewbank, P. C.; Mann, K. R. Introduction of Organic Thin Film Transistors and Design of *n*-Channel Organic Semiconductors. *Chem. Mater*. **2004**, *16*, 4436–4451.

(39) Chen, H. Y.; Chao, I. Effect of Perfluorination on the Charge-Transport Properties of Semiconductors: Density Functional Theory Study of Perfluorinated Pentacene and Sexithiophene. *Chem. Phys. Lett*. **2005,** *401*, 539–545.

(40) Troisi, A. Charge Transport in High Mobility Molecular Semiconductors: Classical Model and New Theories. *Chem. Soc. Rev*. **2011**, *40*, 2347–2358.

(41) Brédas, J. L.; Beljonne, D.; Coropceanu, V.; Cornil, J. Charge-Transfer and Energy-Transfer Process in π-Conjugated Oligomers and Polymers: A Molecular Picture. *Chem. Rev*. **2004**, *104*, 4971–5004.

(42) Coropceanu, V.; André, J. M.; Malagoli, M.; Brédas, J. L. The Role of Vibronic Interactions on Intramolecular and Intermolecular Electron Transfer in π-Conjugated Oligomers. *Theor. Chem. Acc*. **2003**, *110*, 59–69.

(43) Nelsen, S. F.; Yunta, M. J. R. Estimation of Marcus λ for *p*-Phenylenediamines from the Optical Spectrum of a Dimeric Derivative. *J. Phys. Org. Chem.* **1994**, *7*, 55−62.

(44) Nelsen, S. F.; Blackstock, S. C.; Kim, Y. Estimation of Inner Shell Marcus Terms for Amino Nitrogen Compounds by Molecular Orbital Calculations. *J. Am. Chem. Soc.* **1987**, *109*, 677−682.

(45) Wang, L.; Nan, G.; Yang, X.; Peng, Q.; Li, Q.; Shuai, Z. Computational Methods for Design of Organic Materials with High Charge Mobility. *Chem. Soc. Rev*. **2010**, *39*, 423–434.

(46) Viani, L.; Olivier, Y.; Athanasopoulos, S.; da Silva Filho, D. A.; Hulliger, J.; Brédas, J. L.; Gierschener, J.; Cornil, J. Theoretical Characterization of Charge Transport in One-Dimensional Collinear Arrays of Organic Conjugated Molecules. *ChemPhysChem*. **2010**, *11*, 1062–1068.

(47) Chai, S.; Wen, S. H.; Huang, J. D.; Han, K. L. Density Functional Theory Study on Electron and Hole Transport Properties of Organic Pentacene Derivatives with Electron-Withdrawing Substituent. *J. Comput. Chem*. **2011**, *32*, 3218–3225.

(48) Ishii, H.; Sugiyama, K.; Ito, E.; Seki, K. Energy Level Alignment and Interfacial Electronic Structures at Organic/Metal and Organic/Organic Interfaces. *Adv. Mater.* **1999**, *11*, 605–625.

(49) Wang, Y.; Parkin, S. R.; Gierschner, J.; Watson, M. D. Highly Fluorinated Benzobisbenzothiophenes. *Org. Lett.* **2008**, *10*, 3307–3310.

(50) Jones, B. A.; Facchetti, A.; Wasielewski, M. R.; Marks, T. J. Tuning Orbital Energetics in Arylene Diimide Semiconductors. Materials Design for Ambient Stability of *n*-Type Charge Transport. *J. Am. Chem. Soc.* **2007**, *129*, 15259–15278.

(51) Chang, Y. C.; Kuo, M. Y.; Chen, C. P.; Lu, H. F.; Chao, I. On the Air Stability of *n*-Channel Organic Field-Effect Transistors: A Theoretical Study of Adiabatic Electron Affinities of Organic Semiconductors. *J. Phys. Chem. C*. **2010**, *114*, 11595–11601.

(52) Schmidt, R.; Oh, J. H.; Sun, Y. S.; Deppisch, M.; Krause, A. M.; Radacki, K.; Braunscheweig, H.; Konemann, M.; Erk, P.; Bao, Z et al. High-Performance Air-Stable *n*-Channel Organic Thin Film Transistor Based on Halogenated Perylenebismide Semiconductors. *J. Am. Chem. Soc.* **2009**, *131*, 6215–6228.

(53) Becke, A. D. Density-Functional Thermochemistry III. The Role of Exact Exchange. *J. Chem. Phys*. **1993**, *98*, 5648–5652.

(54) Lee, C.; Yang, W.; Parr, R. G. Development of the Colle-Salvetti Correlation-Energy Formula into a Functional of the Electron Density. *Phys. Rev. B*. **1988**, *37*, 785–789.

(55) Zhao, Y.; Truhlar, D. G. The M06 Suite of Density Functionals for Main Group Thermochemistry, Thermochemical Kinetics, Noncovalent Interactions, Excited States, and Transition Elements: Two New Functionals and Systematic Testing of Four M06-Class Functionals and 12 Other Functionals. *Theor. Chem. Acc.* **2008**, *120*, 215–241.

(56) Frisch, M. J.; Trucks, G. W.; Schlegel, H. B.; Scuseria, G. E.; Robb, M. A.; Cheeseman, J. R.; Scalmani, G.; Barone, V.; Mennucci, B.; Petersson, G. A.; et al. GAUSSIAN 09. Revision B.01. Gaussian Inc. Wallingford CT. **2009.**

(57) Vura-Weis, J.; Ratner, M. A.; Wasielewski, M. R. Geometry and Electronic Coupling in Perylenediimide Stacks: Mapping Structure-Charge Transport Relationships. *J. Am. Chem. Soc*. **2010**, *132*, 1738–1739.

(58) Liu, H.; Bremond, E.; Prlj, A.; Gonthier, J. F.; Corminboeuf. C. Adjusting the Local Arrangement of π-Stacked Oligothiophenes through Hydrogen Bonds: A Viable Route To Promote Charge Transfer. *J. Phys. Chem. Lett*. **2014**, *5*, 2320−2324

(59) Hohenstein, E. G.; Chill, S. T.; Sherrill, C. D. Assessment of the Performance of the M05-2X and M06-2X Exchange-Correlation Functionals for Noncovalent Interaction in Biomolecules. *J. Chem. Theory Comput.* **2008**, *4*, 1996–2000.

(60) Jansson, E.; Jha, P. C.; Ågren, H. Density Functional Study of Triazole and Thiadiazole Systems as Electron Transporting Materials. *Chem. Phys*. **2006**, *330*, 166–177.

(61) Dreizler, R. M.; Providência, J. *Density Functional Methods in Physics*, Plenum Press, New York and London, **1985**.

(62) Foresman, J. B.; Frisch, A. E. *Exploring Chemistry with Electronic Structure Methods*, 2nd ed. Pittsburg: Gausssian. Inc. Pittsburgh. **1996**.

(63) Rienstra-Kiracofe, J. C.; Barden, C. J.; Brown, S. T.; Schaefer, H. F. Electron Affinities of Polycyclic Aromatic Hydrocarbons. *J. Phys. Chem*. *A*. **2001**, *105*, 524–528.

(64) Zhan, C. G.; Nichols, J. A.; Dixon, D. A. Ionization Potential, Electron Affinity, Electronegativity, Hardness and Electron Excitation Energy: Molecular Properties from Density Functional Theory Orbital Energies. *J. Phys. Chem. A*. **2003**, *107*, 4184–4195.

(65) Coropceanu, V.; Malagoli, M.; da Silva Filho, D. A.; Gruhn, N. E.; Bill, T. G.; Brédas, J. L. Hole- and Electron-Vibrational Couplings in Oligoacene Crystals: Intramolecular Contributions. *Phys. Rev. Lett*. **2002**, *89*, 275503–275507.

(66) Zhang, G.; Musgrave, C. B. Comparison of DFT Methods for Molecular Orbital Eigenvalue Calculations. *J. Phys. Chem. A*. **2007**, *111*, 1554–1561.

(67) Koh, S. E.; Risko, C.; da Silva Filho, D. A.; Kwon, O.; Fachetti, A.; Brédas, J. L.; Marks, T. J.; Ratner, M. A. Modelling Electron and Hole Transport in Fluoroarene-

Oligothiopene Semiconductors: Investigation of Geometric and Electronic Structure Properties. *Adv. Funct. Mater*. **2008**, *18,* 332−340.

(68) Di Motta, S.; Siracusa, M.; Negri, F. Structural and Thermal Effects on the Charge Transport of Core-Twisted Chlorinated Perylene Bisimide Semiconductors. J. Phys. Chem. C., **2011**, *115*, 20754–20764.

(69) Oxtoby, N. S.; Blake, A. J.; Champness, N. R.; Wilson, C. The Role of 1,2,4,5-Tetrazine Rings in π-π Stacking Interactions. *Cryst. Eng. Comm.* **2003**, *5*, 82−86.

(70) Kurach, E.; Djurado, D.; Rimarčik, J.; Kornet, A.; Wlostowski, M.; Lukeš, V.; Pécaut, J.; Zagorska, M.; Pron, A. Effect of Substituents on Redox, Spectroscopic and Structural Properties of Conjugated Diaryltetrazines − A Combined Experimental and Theoretical Study. *Phys. Chem. Chem. Phys*. **2011**, *13*, 2690−2700.

(71) Geng, Y.; Wang, J.; Wu, S.; Li, H.; Yu, F.; Yang, G.; Gao, H.; Su, Z. Theoretical Discussions on Electron Transport Properties of Perylene Bisimide Derivatives with Different Molecular Packings and Intermolecular Interactions. *J. Mater. Chem*. **2011**, *21*, 134−143.

(72) Geng, Y.; Wu, S. X.; Li, H. B.; Tang, X. D.; Wu, Y.; Su, Z. M.; Liao, Y. A Theoretical Discussion on the Relationships among Molecular Packings, Intermolecular Interactions and Electron Transport Properties for Naphthalene Tetracarboxylic Diimide Derivatives. *J. Mater. Chem*. **2011**, *21*, 15558−15566.

(73) Usta, H.; Facchetti, A.; Marks, T. J. *n*-Channel Semiconductor Materials Design for Organic Complementary Circuits. *Acc. Chem. Res*. **2011**, *44*, 501−510.

(74) Hwang, D. H.; Dasari, R. R.; Fenoll, M.; Alain-Rizzo, V.; Dindar, A.; Shim, J. W.; Deb, N.; Fuentes-Hernández, C.; Barlow, S.; Bucknall, D. G.; et al. Stable

Solution-Processed Molecular *n*-Channel Organic Field-Effect Transistors. *Adv. Mater.* **2012**, *24*, 4445–4450.

(75) Davids, P. S.; Campbell, I. H.; Smith, D. L. Device Model for Single Carrier Organic Diodes. *J. Appl. Phys.* **1997**, *82*, 6319–6325.

(76) Al Attar, H. A.; Monkman, A. P. Dopant Effect on the Charge Injection, Transport and Devices Efficiency of an Electrophosphorescent Polymeric Light-Emitting Device. *Adv. Funct. Mater.* **2006**, *16*, 2231–2242.

(77) Amy, F.; Chan, C.; Kahn, A. Polarization at the Gold/Pentacene Interface. *Org. Electron.* **2005**, *6*, 85–91.

(78) Crispin, X.; Geskin, V.; Crispin, A.; Cornil, J.; Lazzaroni, R.; Salaneck, W. R.; Brédas. J. L. Characterization of the Interface Dipole at Organic/Metal Interfaces. *J. Am. Chem. Soc*. **2002**, *124*, 8131–8141.

(79) Cheng, X.; Noh, Y. Y.; Wang, J.; Tello, M.; Frisch, J.; Blum, R. P.; Vollmer, A.; Rabe, J. P.; Koch, N. T.; Sirringhaus, H. Controlling Electron and Hole Charge Injection in Ambipolar Organic Field-Effect Transistors by Self-Assembled Monolayers. *Adv. Funct. Mater*. **2009**, *19*, 2407–2415.

(80) Wen, Y.; Liu, Y. Recent Progress in *n*-Channel Organic Thin-Film Transistors. *Adv. Mater*. **2010**, *22*, 1331–1345.

(81) Yan, L.; Zhao, Y.; Wang, X.; Wang, X. Z.; Wong, W. Y.; Liu, Y.; Wu, W.; Xiao, Q.; Wang, G.; Zhou, X.; et al. Platinum-Based Poly(aryleneethynylene) Polymers Containing Thiazolothiazole Group with High Hole Mobilities for Field-Effect Transistors Applications. *Macromol. Rapid Commun*. **2012**, *33*, 603–609.

(82) De Leeuw, D. M.; Simenon, M. M. J.; Brown, A. R.; Einerhand, R. E. F. Stability of *n*-Type Doped Conducting Polymers and Consequences for Polymeric Microelectronic Devices. *Synth. Met.*, **1997**, *97*, 53–59.

(83) Kuo, M. Y.; Chen, H. Y.; Chao, I. Cyanation: Providing a Three-In-One Advantage for the Design of *n*-Type Organic Field-Effect Transistors. *Chem. Eur. J.* **2007**, *13*, 4750–4758.

(84) Meng, Q.; Hu, W. Recent Progress of *n*-Type Organic Semiconducting Small Molecules for Organic Field-Effect Transistors. *Phys. Chem. Chem. Phys.* **2012**, *14*, 14152–14164.

(85) CRC, *Handbook of Chemistry and Physics*, CRS Press, Boca Raton, FL, **1995**.

(86) Yasuda, T.; Goto, T.; Fujita, K.; Tsutsui, T. Ambipolar Pentacene Field-Effect Transistors with Calcium Source-Drain Electrode. *Appl. Phys. Lett.* **2004**, *11*, 2098–2100.

(87) Koch, N.; Zojer, E.; Rajagopal, A.; Ghjsen, J.; Johnson, R. L.; Leising, G.; Pireaux, J. J. Electronic Properties of the Interface between the Wide Bandgap Organic Semiconductors *para*-Sexiphenyl and Samarium. Adv. *Funct. Mater.* **2001**, *11*, 51–58.

(88) Stössel, M.; Staudigle, J.; Steuber, F.; Simmerer, J.; Winnacker, A. Impact of the Cathode Metal Work Function on the Performance of Vacuum-Deposited Organic Light Emitting-Devices. *Appl. Phys. A.* **1999**, *68*, 387–390.

(89) Michaelson, H. B. The Work Function of the Elements and its Periodicity. *J. Appl. Phys*. **1977,** *48*, 4729−4733.

(90) Sze, S. M. *Physics of Semiconductor Devices* (Wiley, New York **1981**).

(91) Zhou, Q.; Audebert, P.; Clavier, G.; Méallet-Renault, R.; Miomandre, F.; Shaukat, Z.; Vu, T. T.; Tang, J. New Tetrazines Functionalized with Electrochemically and Optically Active Groups: Electrochemical and Photoluminescence Properties. *J. Phys. Chem. C.* **2011**, *115*, 21899–21906.

(92) Audebert, P.; Sadki, S.; Miomandre, F.; Clavier, F.; Vernières, M. C.; Saoud, M.; Hapiot, P. Synthesis of New Substituted Tetrazines: Electrochemical and Spectroscopy Properties. *New J. Chem.*, **2004**, *28*, 387–392.

(93) Qing, Z.; Audeber, P.; Clavier, G.; Miomandre, F.; Tang, J.; Vu, T. T.; Méallet-Renault, R. Tetrazines with Hindered or Electron Withdrawing Substituents: Synthesis, Electrochemical and Fluorescence Properties. *J. Electroanal. Chem.,* **2009**, *632*, 39–44.

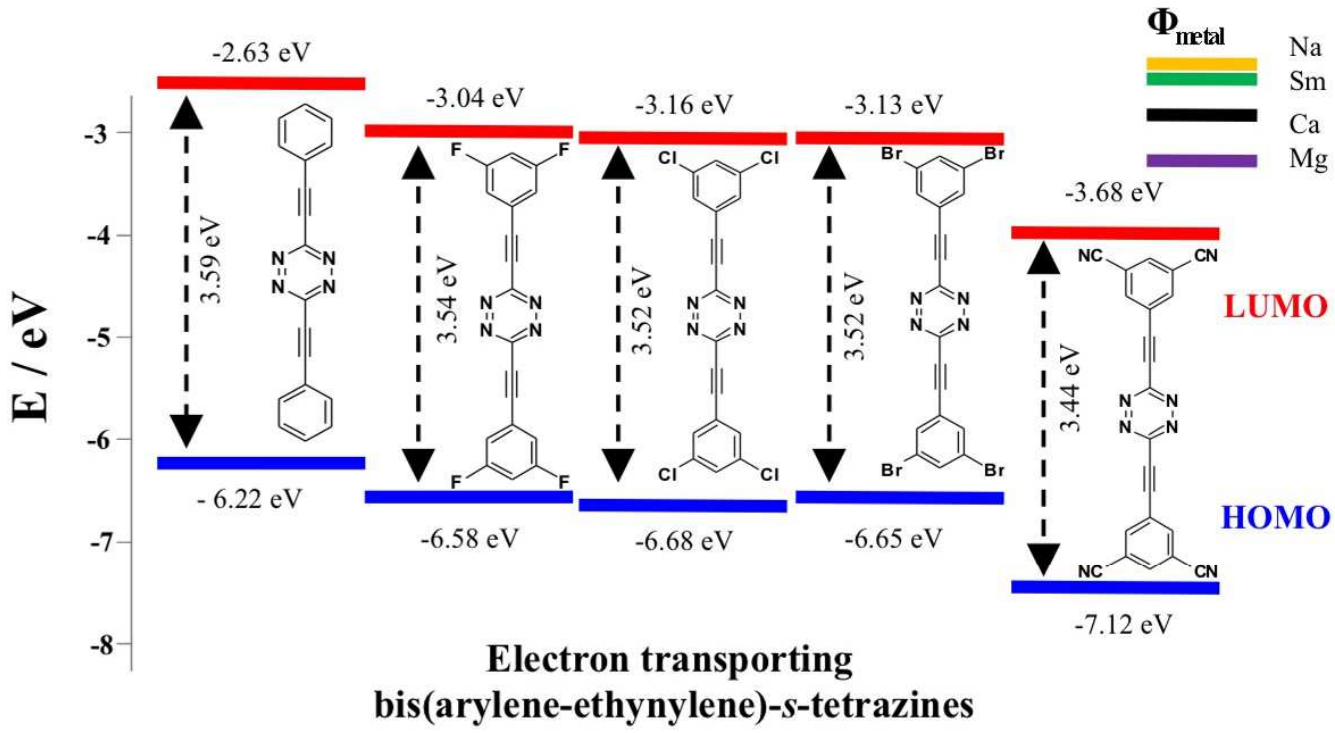

Electron transporting bis(arylene-ethynylene)-*s*-tetrazines